Finite Computational Models of Iterated Maps

NAU 2010 Summer REU Report

Bryan Crompton

August 12, 2010

Abstract

Iterated maps exhibit rich dynamical behavior. However, the theoretical behavior of such maps is different than the computed behavior on inherently finite machines. A finite computational model is studied in this paper using the logistic map. Because the approximating set is finite, each point can be labeled and there is an associated directed graph. Properties of the directed graph are studied in general, at bifurcation points of the logistic map, and at $a = 4$ chaos in the logistic map. Additionally, error statistics involved are briefly examined.

1 Introduction

Consider a one-dimensional iterated map $f : [0,1] \to [0,1]$. The map over the unit interval can be approximated by $N+1$ points, that is the set of rational numbers $\{0, 1/N, 2/N, \ldots, 1\}$, in the following way. Since all points have a common denominator, let the integer k be synonymous with the point k/N. For each N define the map $F_N : \mathbf{Z}_{N+1} \to \mathbf{Z}_{N+1}$ as

$$F_N(k) = R[N \cdot f(k/N)], \tag{1}$$

where $R : [0,N] \to \mathbf{Z}_{N+1}$ is some rounding function. Now consider the iterated map $k_{n+1} = F(k_n)$. It is of interest to consider how the "true" sequence $x_0, x_1, x_2, \ldots$ defined by $x_{n+1} = f(x_n)$ compares with the sequence $k_0/N, k_1/N, k_2/N, \ldots$.

The approximation method intends to capture the finite computational nature of calculating orbits of iterated maps. Specifically, it models fixed precision computations. However, on most computers, the IEEE standard of double precision (DP) for representing decimals is used. Double precision is a floating point approximation and the spacing between adjacent points is not uniform. A more general model might be then

$$F_N(k) = R[(h_N^{-1} \circ f \circ h_N)(k)] \tag{2}$$

where $h_N : [0,N] \to [0,1]$ is a monotonic, continuous bijection. The fixed point model corresponds to $h_N(k) = k/N$. Another interesting case would be one that avoids $x = 0$ or $h_N(k) = (k+0.5)/(N+1)$. In all cases, periodic orbits must exist because the approximating set is finite. For double precision, large numerically induced periods on the order of 10^7 are observed when computing orbits of the logistic map at $a = 4$. Systematically studying the behavior of the orbits using simpler fixed point approximation schemes has the potential to give greater insight into behavior such as this.

Figure 1: Directed Graph of Logistic Map for $a = 4$ and $N = 32$.

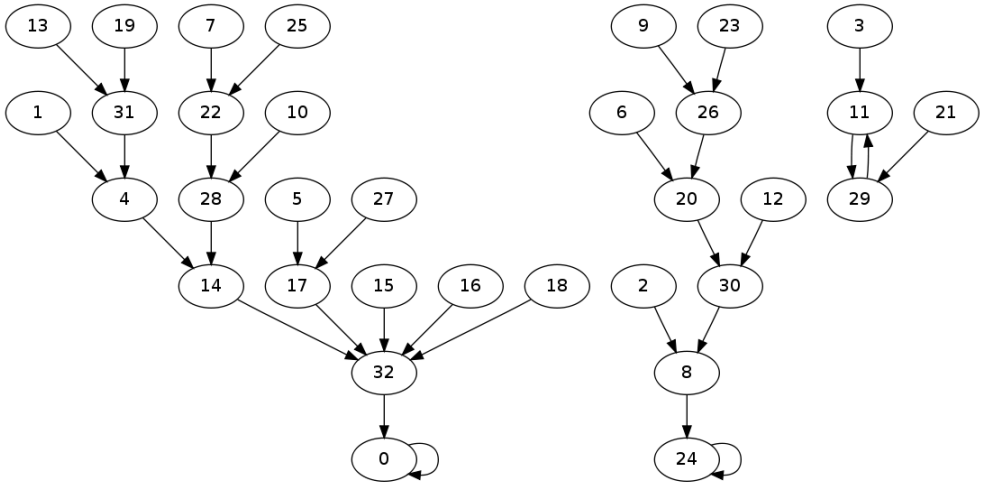

For each F_N, there is an associated directed graph. See Figure 1 for an example. Each number in the set $\{0, 1, 2, \ldots, N\}$ is a node and an arrow is drawn from a node $j \to k$ if $k = F_N(j)$. A node k is *non-invertible* if there does not exist a j such that $k = F_N(j)$. In other words, no arrows go into it. For example, the nodes 13, 19, 7 and 25 are non-invertible in Figure 1. A *periodic orbit* is a set

$\{k_1, k_2, \ldots, k_n\}$ such that $F_N^{(n)}(k_i) = k_i$ for each $1 \leq i \leq n$. If n is the smallest n such that this occurs, then it is called the minimal period or just the period of the orbit. Periodic orbits in Figure 1 are $\{0\}$, $\{24\}$, and $\{11, 29\}$. The *basin of a periodic orbit* is the set of all nodes that eventually end up in that periodic orbit. In Figure 1 there are three basins.

Since each orbit is periodic or eventually periodic, for an initial point k, define $P(k)$ to be the eventual periodic orbit and $T(k)$ to be the transient. Let $p(k)$ be the minimal period and $t(k)$ the length of the transient. For example, in Figure 1 the initial point $k = 31$ has the orbit

$$31, 4, 14, 32, 0, 0, 0, \ldots.$$

Thus, $P(31) = \{0\}$, $p(31) = 1$, $T(31) = \{31, 4, 13, 32\}$, and $t(31) = 4$. The *depth of the basin* is the largest $t(k)$ in the basin. The leftmost basin in Figure 1 has a depth of 5.

The properties of the directed graph should be studied as parameters such as N are varied. There is some expectation that as $N \to \infty$, the orbit will be more and more behaved as it would be theoretically. In full generality, the number of points N, the rounding scheme, the positioning of the points h_N, and the iterated map (such as a parameter family) can all be varied and the properties of the directed graph studied. Again, these properties include the number of basins, the size of the basins, the periodic orbits, and the average transients. One more note about rounding. The function $R(x)$ may round to the nearest integer, it may round up, or it may round down. Additionally, it may round pseudo-randomly. It is possibly worth investigating this last possibility because rounding is not consistent from machine to machine using floating point arithmetic.

This paper will focus on the logistic map $f(x) = ax(1 - x)$ at the first bifurcation point $a = 3$ and $a = 4$. Additionally, it will look at some of the error statistics involved in the finite approximation.

2 General Properties of Model

2.1 Existence of Fixed Points

Consider the logistic map $f(x) = ax(1-x)$ under the model of equation (1) with the "round to nearest" function. A fixed point k of F_N must satisfy

$$k = R(Nf(k/N)) = R\left[\frac{ak(N-k)}{N}\right] = \frac{ak(N-k)}{N} + \epsilon$$

where $|\epsilon| \leq 1/2$. Solving for ϵ and using the inequality, we conclude all fixed points must satisfy

$$\left|\frac{ak^2 + (1-a)k}{N}\right| \leq 1/2 \quad \text{or} \quad \left|ak^2 + (1-a)Nk\right| \leq N/2.$$

Let $H(k) = ak^2 + (1-a)Nk$. Then solving $H(k) = \pm 1/2$ gives

$$k = \frac{a-1}{2a}N\left(1 \pm \sqrt{1 \pm \frac{2a}{(a-1)^2 N}}\right)$$

or using the binomial expansion

$$k \approx \pm\left(\frac{1}{2(a-1)} + O(1/N)\right) \quad \text{or} \quad k \approx (1-\frac{1}{a})N \pm \left(\frac{1}{2(a-1)} + O(1/N)\right).$$

This means integer solutions to the inequality must exist in

$$\left[-\frac{1}{2(a-1)} - O\left(\frac{1}{N}\right), \frac{1}{2(a-1)} + O\left(\frac{1}{N}\right)\right],$$

and

$$\left[(1-\frac{1}{a})N - \frac{1}{2(a-1)} - O\left(\frac{1}{N}\right), (1-\frac{1}{a})N + \frac{1}{2(a-1)} + O\left(\frac{1}{N}\right)\right].$$

It is clear that $k = 0$ is an integer solution that always satisfies the inequality. When $a > 3/2$, we have $\frac{1}{2(a-1)} + O(1/N) < 1$ for sufficiently large N, ruling out any other possible integer solutions near 0 for this case.

Now suppose $a = 3$ or $a = 4$. Then

$$(1 - 1/a)N = m + r/a,$$

where m is some integer and r is some positive integer such that $r < a$. The nearest integers are then

$$(1 - 1/a)N - r/a \text{ and } (1 - 1/a)N + (1 - r/a).$$

For an integer solution to exist, we must have $r/a < \frac{1}{2(a-1)} + O(1/N)$ in the first case and $1 - r/a < \frac{1}{2(a-1)} + O(1/N)$ in the second. If we require $\frac{a}{2(a-1)} + O(1/N) < 1$, then we force $r < 1$ and $a - r < 1$. If this occurs, then we can only have integers solutions when $r = 0$, or N is a multiple of a. For large enough N, for $a = 3$ we get $3/(2 * (3-1)) + O(1/N) = 3/4 + O(1/N)$ and for $a = 4$ we get $4/(2 * (4-1)) + O(1/N) = 4/6 + O(1/N) < 1$.

In summary, we can only have a fixed point if N is a multiple of a when $a = 3$ and $a = 4$.

3 Orbits of the Logistic Map at $a = 3$

Consider the use of Equation (1) for the logistic map at $a = 3$ and with rounding to the nearest integer. How does the finite representation of the unit interval affect computations of orbits near bifurcation points? Theoretically, all points in $(0, 1)$ converge to $x = 2/3$ (see Theorem 1). With the approximation model, will all points in the set $\{1, 2, \ldots, N\}$ end up at a fixed point $k = R(2N/3)$?

Computations show that instead of all trajectories heading to a single point, they head to multiple different small period 2 orbits which cluster around the approximate fixed point. As the parameter N is increased, the number of basins for period two orbits increase as well. In general, the directed graph associated to the finite map with $a = 3$ and for any N has the following features. See Figure 2 for the particular case $N = 64$. First, there is of course, the trivial orbit $N \to 0$. Because the maximum of $f_3(a)$ is $3/4$, no k is mapped by F_N to N. Thus, no other points are included in this orbit. Second, there are multiple period two orbits with values close to the approximate fixed point $k^* = [2/3N]$ roughly in the form $(k^* - j, k^* + j)$ for some almost consecutive sequence $j = 1, 2, 3, \ldots, n$. Finally, the total number of points heading to each period two orbit is not the same. One basin many orders of magnitude larger than the others has been observed. The periodic orbit associated with this basin has always been observed to the one farthest from the fixed point.

Figure 2: Directed Graph of Logistic Map for $a = 3$ and $N = 64$.

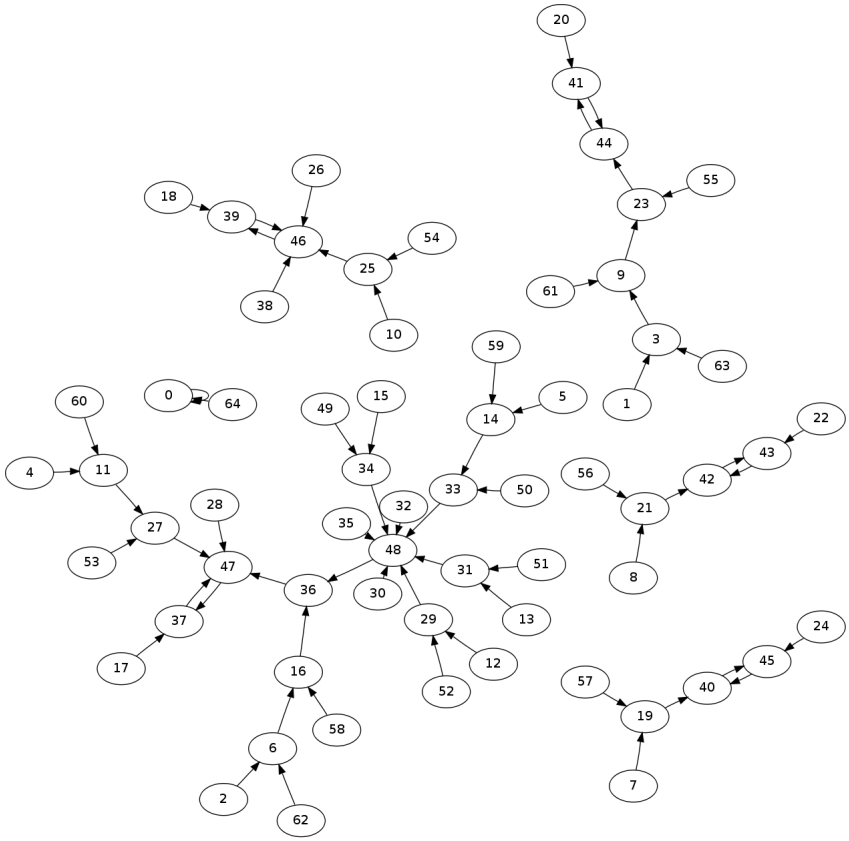

3.1 Number of Basins

Let $b(N)$ be the number of basins in the directed graph associated with F_N. Figures 3 and 4 show $b(N)$ vs. N and $\log b(N)$ vs. $\log N$.

Figure 3: Number of Basins vs. N

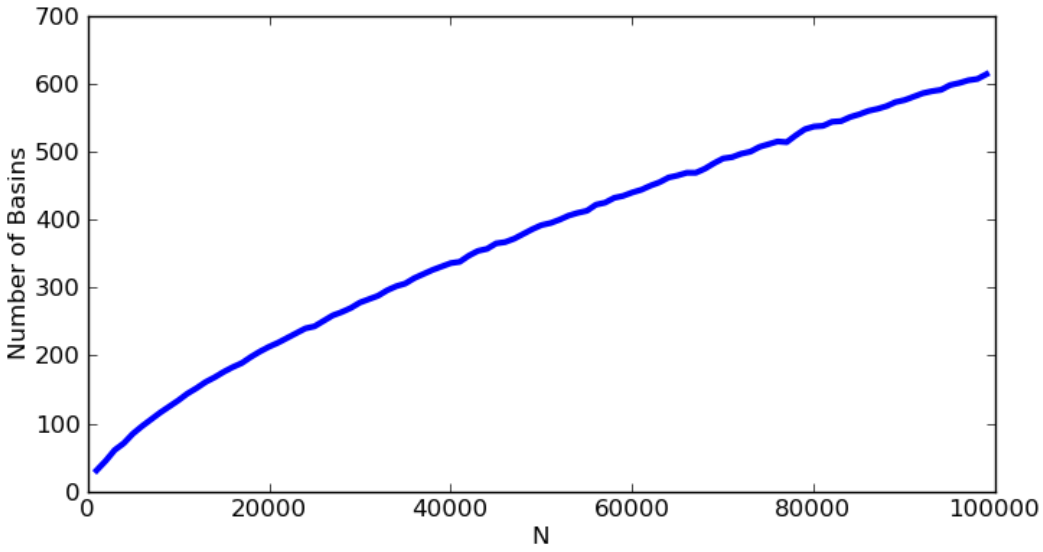

Figure 4: Log of Number of Basins vs. Log of N

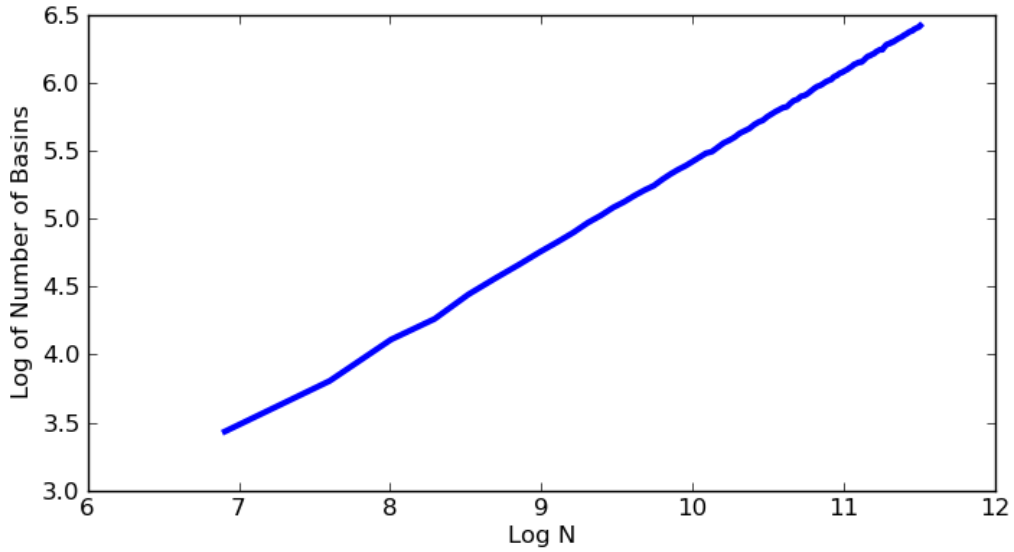

The linearity of the curve in Figure 4 suggests $B(N)$ obeys a power law. A linear fit gives

$$\log b(N) = 0.6632 \log N - 1.2092,$$

or equivalently

$$b(N) = 0.2984N^{0.6632}, \tag{3}$$

with an r^2 value of 0.9999077.

A possible explanation of this is that near the fixed point $2N/3$, the second iterate gets rounded to the 45 degree line for a range of values. Specifically, if the difference $f^2(x) - x$ is small enough, then it is likely that for k with $x = k/N$, it will be a periodic point. It can be shown that

$$f^2(x) - x = -x(1 - a + ax)(1 + a - ax - a^2x + a^2x)$$

and for $a = 3$, this is

$$f^2(x) - x = -x(-2 + 3x)(4 - 12x + 9x).$$

The region around the fixed point is what is important, so substitute $y = x - 2/3$ and let $E(y) = f^2(x) - x$ to get

$$\begin{aligned} E(y) &= -(y + 2/3)(-2 + 3y + 2)(4 - 12y - 8 + 9(y^2 + 4/3y + 4/9)) \\ E(y) &= -27y^3(y + 2/3) \\ E(y) &= -(18y^3 + 27y^4). \end{aligned}$$

For small y the 4th order term is neglible. It is likely that only when $|E(y)| < 1/2N$ is it possible for there to be a rounded period two orbit. After one iteration of the finite map, if the difference $f(x) - x$ is greater than $1/2N$, its impossible for it to get rounded to a fixed point (using the typical rounding scheme). It is assumed that this is the same for the second iterate, even though the errors are more complicated. A better argument could perhaps be made by examining the distribution of round-off errors that occur after two iterations. Regardless, using this assumption, the approximate region where we can have rounded period two orbits is given by

$$18|y|^3 < \frac{1}{2N}$$

implying that

$$|y| < \frac{1}{\sqrt[3]{36N}} \approx 0.3028\frac{1}{\sqrt[3]{N}}. \tag{4}$$

Thus, roughly the total number of period 2 basins is N times the right hand side or

$$b(N) \approx 0.3028N^{2/3}. \tag{5}$$

Technically, the trivial closed basin $N \to 0$ also always exists, so additional term of 1 should be added. But for large N, this is unnoticeable. The formula derived is in remarkable argreement with the empirical fit. The leading constant in the linear fit is 0.2984, less than the predicted 0.3028 by 0.0044 or 1.5%.

3.2 Size and Locations of Basins.

The reasoning in the previous section suggests that period two orbits cluster around the $2N/3$ fixed point. A natural question is what is the size of each basin? Figure 5 shows a distribution typical of any N. It plots the maximum value in each periodic orbit with the size of the basin. The relative sizes of each basin vary greatly, so the natural log is taken in order for the features of the distribution to be noticed. There are a couple of features to note. First, the rightmost periodic orbit, the one farthest away from the fixed point $k = 33,333$, is larger than all the others by several orders of magnitude. Second, there is a sort of layered structure. There appears a dense uniform distribution of very small basins, and then a slightly less dense uniform distribution of incrementally larger basins superimposed on the same region, and so on for about a total of five iterations. Third, there is a sequence of large basins leading up to the rightmost basin that breaks this trend. Finally, there are some gaps between basins the farther away from the fixed point. An explanation of these effects would be desirable.

Figure 5: Basin Distribution for $N = 50,000$

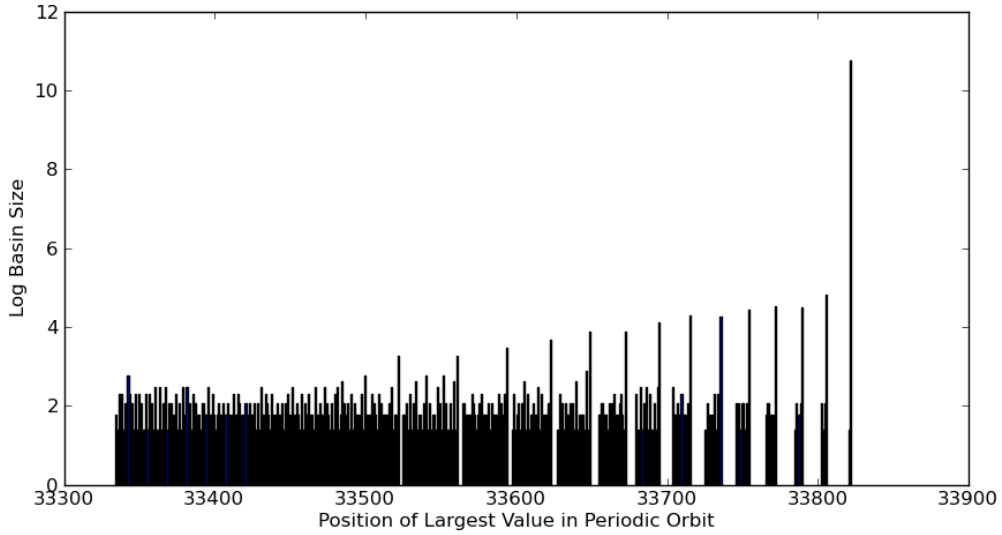

Another natural question that arises is where does each initial point end up? Figure 6 graphs each initial point with the first value it hits in an periodic orbit with $N = 50,000$. The trival orbit is ignored in order for the graph to display meaningful data.

Figure 6: Orbit Limits for $N = 50,000$

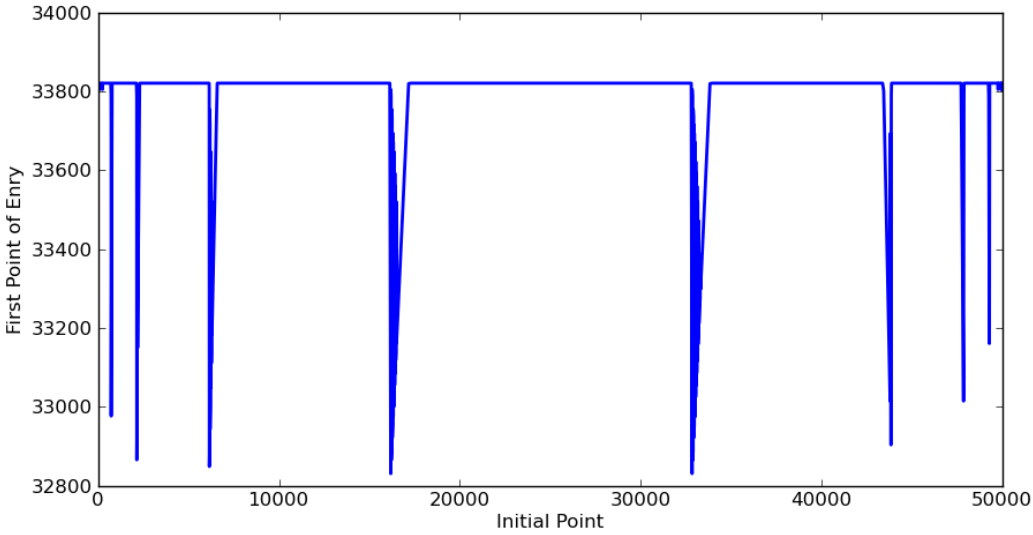

The plot is reminiscent of large iterates of $f(x)$. For example, Figure 7 shows the 50th iterate of f. The flat regions and the sloped regions appear to align in Figures 6 and 7. This suggests the limiting behavior of the iterates of f influences the distribution of the basins.

Figure 7: 50th iterate

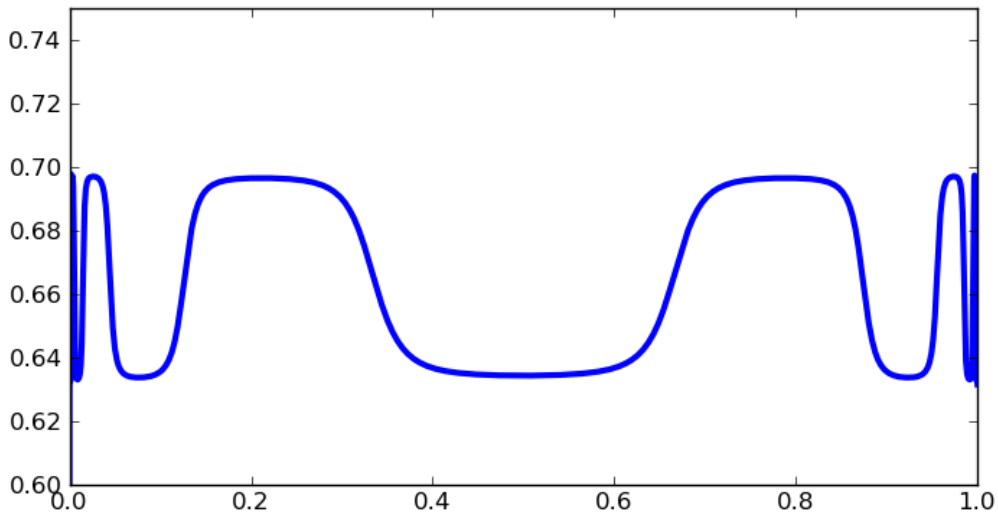

Looking at the derivatives of the 50th and higher iterates (see Figure 8 for a graph of the derivative of 50th iterate) suggests that $\lim_{n\to\infty} f^{(n)'}(x) = 0$ except for select values. More careful study suggests

the following conjecture.

Conjecture 1. For all $x \in (0,1) - \cup_{n=1}^{\infty} f^{(-n)}(2/3)$, that is all points not in the pre-orbit of the fixed point, $\lim_{n\to\infty} |f^{(n)'}(x)| = 0$. Otherwise, for $x \in \cup_{n=1}^{\infty} f^{(-n)}(2/3)$, the limit is non-zero.

In fact, the points in the preorbit of the fixed point appear to have a constant slope after some finite number of iterates.

Figure 8: Plot of $|f^{(50)'}(x)|$

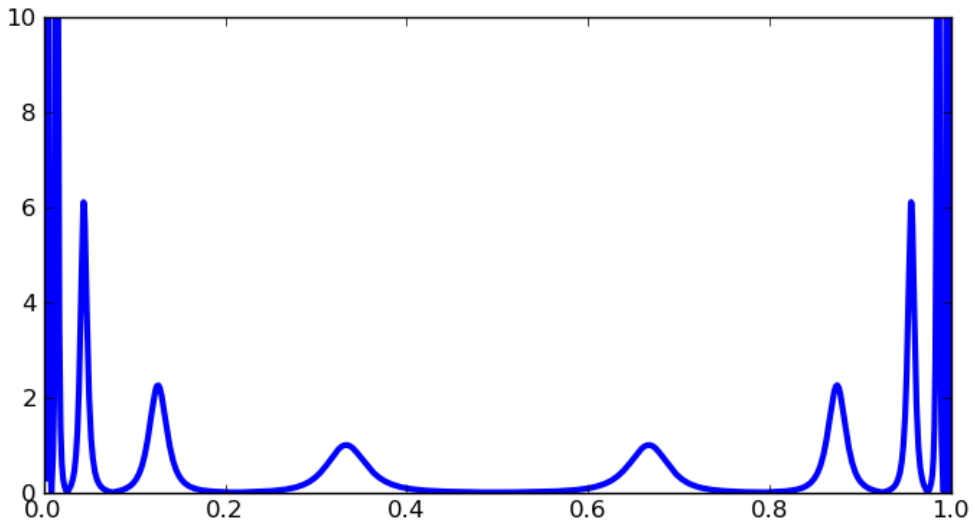

The existence of the limit $\lim_{n\to\infty} |f^{(n)'}(x)|$ is proven later on in this paper. Unfortunately, the conjecture has turned out difficult to prove.

Eventually, the iterates of the finite logistic map are going to be periodic. It is then reasonable to assume that they approximate some large iterate of the true map. Thus, the limiting behavior of the map is important and this is why it is important that the limit of the derivative exists. It turns out it can explain the characteristics of the graph in Figure 5. First, since the slope at most of the regions gets really small and perhaps approaches zero, this accounts for why there is a large basin. Second, the different sloped regions that remain fixed account account for the layered uniform distribution. The slopes at 1/3 and 2/3 are roughly one. This means that rounding will contribute points to each periodic basin equally. However, the next pair of points in the pre-orbit have a greater slope near 2. Due to rounding, this means that every other basin will get additional points. The sequence of different sloped regions continues on, accounting for the roughly the five different layered distributions. Third, the regions between the sloped parts and the flat parts in the approximate iterate account for the increasing sequence leading up to the largest basin.

If Conjecture 1 is true, then the larger the iterate, the greater the flat regions will become. It is natural to think that as N increases, it approximates larger iterates more accurately. This suggests that the fraction of the total graph of the will approach one. Figure 9 verifies this suspicion by showing the relative size of the largest basin versus N.

Figure 9: Percentage Largest Basin Takes Up

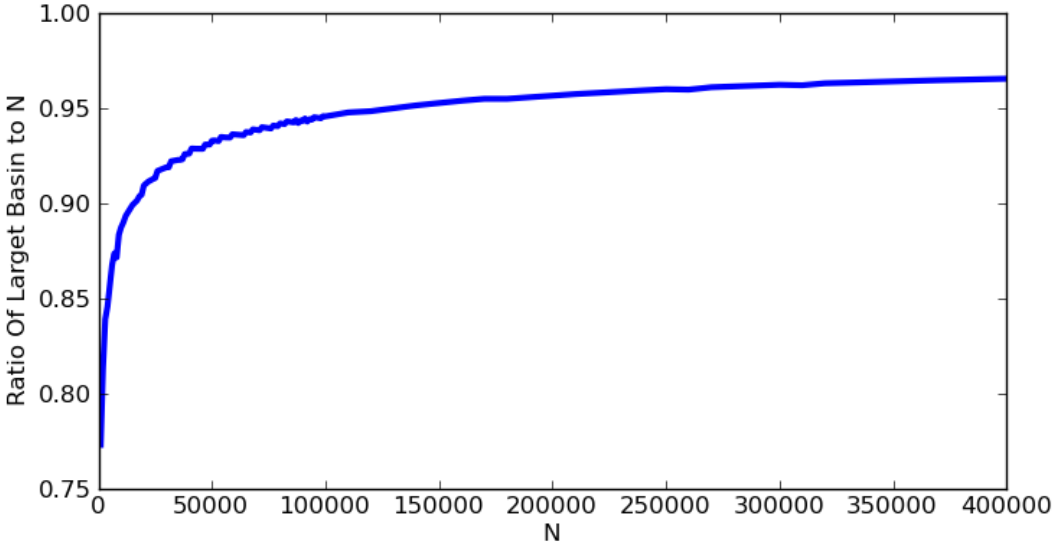

3.3 Analysis for $a = 3$

Lemma 1. Let $f : I \to I$ be a continuous iterated map and suppose for some $x \in I$, $\lim_{n\to\infty} f^{(n)}(x) = L$. Then the limit L must be a fixed point of f.

Proof. By the continuity of f,

$$f(L) = f\left(\lim_{n\to\infty} f^{(n)}(x)\right) = \lim_{n\to\infty} f^{(n+1)}(x) = \lim_{n\to\infty} f^{(n)}(x) = L.$$

Hence L is a fixed point. ■

Theorem 1. Let $f(x) = 3x(1-x)$. Then for $x \in (0,1)$, $\lim_{n\to\infty} f^{(n)}(x) = 2/3$.

Proof. This proof will first show that for $x \in [1/2, 2/3]$ the limit is $2/3$. Then, it will show that the orbits of all $x \in (0,1)$ end up in $[1/2, 2/3]$, from which the theorem follows.

Claim 1.1 For $x \in [1/2, 2/3]$, we have $\lim_{n\to\infty} f^{(n)}(x) = 2/3$.

Define the sequence $y_n = x_n - 2/3$. The map of its second iterate is $g(y) = f^{(2)}(x) - 2/3 = f^{(2)}(y + 2/3) - 2/3 = -27y^4 - 18y^3 + y$, as shown in Section 3.1. Let $I = [-1/6, 0]$. It will be demonstrated that $g(y)$ is monotonic on I, that $g(I) \subseteq I$, and that $g(y) > y$ on I.

Consider

$$g'(y) = -108y^3 - 54y^2 + 1 = (y + \frac{1}{6})(-108y^2 - 36y + 6).$$

Application of the quadratic formula reveals that the other roots are $-\frac{1}{6}\left(1 \pm \sqrt{3}\right)$. Because $\sqrt{3} > 1$, we know that know no other roots of g', and hence no other extrema, exist in I. Thus, g is monotonic on I. Because g is monotonic, we have

$$g\left(I\right) = \left[g\left(-\frac{1}{6}\right),\ g(0)\right] = \left[-\frac{5}{48},\ 0\right] \subseteq I.$$

It is easily shown that $g(y) - y$ has zeros at 0 and $-2/3$, so it has the same sign on I. Calculating $g(-1/6) - (-1/6) = -5/48 + 1/6 = 1/16 \geq 0$ demonstrates that $g(y) \geq y$ on I.

The last two of the three properties of g just shown imply that $g^{(n)}(y)$ with $y \in I$ remains in I and is increasing. It is also bounded by $1/3$. We conclude that the limit exists, and must be a fixed point of $g(y)$, which was already shown to be $-2/3$ or 0. It cannot be $-2/3$ since the sequence is increasing and starts in I. Thus, the limit is 0.

Since $\lim_{n\to\infty} g^{(n)}(y) = 0$ for $y \in [-1/6, 0]$, it follows that $\lim_{n\to\infty} f^{(2n)}(x) = 2/3$ for $x \in [1/2, 2/3]$. By the continuity of f, we must also have

$$f\left(\lim_{n\to\infty} f^{(2n)}(x)\right) = \lim_{n\to\infty} f^{(2n+1)}(x) = f(2/3) = 2/3.$$

The claim that $\lim_{n\to\infty} f^{(n)}(x) = \frac{2}{3}$ for $x \in [1/2, 2/3]$ follows from this. ■

Claim 1.2 The expression $(0,1) \subseteq \cup_{n=0}^{\infty} f^{(-n)}([1/2, 2/3])$ holds.

Calculations reveal that $f^{(2)}([1/3, 2/3]) = f([2/3, 3/4]) = [9/16, 2/3] \subseteq [1/2, 2/3]$. This means $\cup_{n=0}^{\infty} f^{(-n)}([1/3, 2/3]) \subseteq \cup_{n=0}^{\infty} f^{(-n)}([1/2, 2/3])$. Let $g(y) = \frac{1}{2} - \frac{1}{6}\sqrt{9 - 12y}$, satisfying $f(g(y)) = y$ for $y \in [0, 3/4]$. This implies by induction $f^{(-n)}([1/3, 2/3]) \subseteq [g^{(n)}(1/3), 1 - g^{(n)}(1/3)]$. The case $n = 0$ is obvious. Then

$$f^{(-n-1)}([1/3, 2/3]) \subseteq f^{-1}([g^{(n)}(1/3), 1 - g^{(n)}(1/3)]) = [g^{(n+1)}(1/3), 1 - g^{(n+1)}(1/3)],$$

since $g^{(n)}(1/3) < 1/4$ for $n \geq 1$ as will be shown. This means $3/4$ is always in the interval for $n \geq 1$, so the preimage of the iterval is also an interval (and not two).

Because $g(y)$ is concave up on $[0, 3/4]$ and $g(3/4) = 1/2$ and $g(0) = 0$, we have $y > g(3/4)y = y/2 > g(y)$ on that interval. This means that $g^{(n)}(1/2)$ is decreasing. It is also bounded, and hence it has a limit. The limit must be the fixed point $y = 0$ of $g(y)$. Choosing any $x \in (0, 1)$, we can always find an N making $g^{(n)}$ small enough such that $x \in [g^{(n)}(1/3), 1 - g^{(n)}(1/3)] = f^{(-n)}([1/3, 2/3])$. This shows that $(0, 1) \subseteq \cup_{n=0}^{\infty} f^{(-n)}([1/3, 2/3]) \subseteq \cup_{n=0}^{\infty} f^{(-n)}([1/2, 2/3])$. ■

By Claim 1.2, for all $x \in (0, 1)$ there is an m such that $f^{(m)}(x) \in [1/2, 2/3]$. By Claim 1.1, this implies that $\lim_{n\to\infty} f^{(n+m)}(x) = \lim_{n\to\infty} f^{(n)}(x) = 2/3$. This completes the proof of the theorem. ■

Theorem 2. Let $f(x) = 3x(1 - x)$. Then $\lim_{n\to\infty} |f^{(n)'}(x)|$ exists for $x \in (0, 1)$.

Proof. This proof uses the fact that for all $x \in (0, 1)$, we have $\lim_{n\to\infty} x_n = 2/3$. First, note that by the chain rule

$$|f^{(n)'}(x)| = \prod_{k=0}^{n-1} |f'(f^{(k)}(x))|,$$

so for convience let $b_k(x) = |f'(f^{(k)}(x))|$ and $a_n(x) = |f^{(n)'}(x)| = \prod_{k=0}^{n-1} b_k(x)$. It will be shown that $\lim_{n\to\infty} a_n(x)$ exists for $x \in (0, 1)$.

Claim 2.1. Let $I = [\frac{1}{2} - \frac{\sqrt{3}}{6}, \frac{1}{2} + \frac{\sqrt{3}}{6}]$. Then $f(I) \subseteq I$ and $|f'(x)f'(f(x))| \leq 1$ on I.

Proof. We compute

$$h(x) = f'(x)f'(f(x)) = 9(1 - 2x)(1 - 6x + 6x^2)$$

and note it is a cubic with zeros at $x = 1/2$ and $x = 1/2 \pm \sqrt{3}/6$. Solutions of $h'(x) = 0$ are $x = 1/3, 2/3$, at which $h(x)$ obtains values of $+1$ and -1 respectively. Thus, on the interval $I = [1/2 - \sqrt{3}/6, 1/2 + \sqrt{3}/6]$ we have $|h(x)| \leq 1$ and strictly less than 1 on $I - \{1/3, 2/3\}$. It is a straightforward calculation to show that

$$f(I) = (2/3, 3/4] \subseteq I,$$

and hence the lemma is proved.

Claim 2.2. The limits of $a_{2n}(x)$ and $a_{2n+1}(x)$ exist on I.

Proof. Since by Claim 2.1 we have $f(I) \subseteq I$, for all initial points $x \in I$ the orbit remains in I. Thus we have $b_k(x)b_{k+1}(x) = |f'(x)f'(f(x))| = |h(x)| \leq 1$. This implies

$$a_{n+2}(x) = a_n(x)\ b_n(x)\ b_{n+1}(x) \leq a_n(x).$$

The sequences are obviously bounded by zero, and since they are also monotonically decreasing, the limits of $a_{2n}(x)$ and $a_{2n+1}(x)$ must exist, demonstrating the lemma.

Now to show $\lim a_n(x)$ exists on I. Define $c_k(x) = 1$ if k is odd otherwise let $c_k(x) = b_k(x)$. Note by the continuity of $f'(x)$, we have $\lim b_k(x) = \lim |f'(x_k)| = |f'(\lim x_k)| = |f'(2/3)| = 1$, which implies the limit of $c_k(x)$ is also 1. Then

$$a_n(x) = a_{2\lfloor n/2 \rfloor}(x)\ c_{n-1}(x),$$

implying by limit laws that the limit $a_n(x)$ exists on I and is the same as $a_{2n}(x)$ and $a_{2n-1}(x)$ on I.

Since for $x \in (0, 1)$ we have $\lim_{n\to\infty} x_n = 2/3$, there is an m such that $x_m \in (2/3 - \epsilon, 2/3 + \epsilon) \subseteq I$, where $x_m = f^{(m)}(x) \in I$. It is true that

$$a_{n+m}(x) = a_m(x)\ a_n(x_m).$$

By Claim 2.2 $\lim_{n\to\infty} a_n(x')$ exists, and since $a_m(x)$ is constant, we conclude $\lim_{n\to\infty} a_{n+m}(x) = \lim_{n\to\infty} a_n(x)$ exists. This proves the theorem. ■

The following conjecture was made.

Conjecture 1. For all $x \in (0,1) - \cup_{n=1}^{\infty} f^{(-n)}(\{2/3\})$, that is all points not in the pre-orbit of the fixed point, $\lim_{n\to\infty} |f^{(n)'}(x)| = 0$. Otherwise, for $x \in \cup_{n=1}^{\infty} f^{(-n)}(\{2/3\})$, the limit is non-zero.

It is easy to show that $x \in \cup_{n=1}^{\infty} f^{(-n)}(2/3)$ implies the limit is non-zero. This is because there is a $M \in \mathbf{N}$ such that $|f'(x_n)| = |f'(2/3)| = 1$ for all $n \geq M$ since $x_n = 2/3$ for $n \geq M$, so the limit is $\prod_{k=0}^{M-1} |f'(f^k(x))|$. If this is zero, then the orbit of x would have to hit $1/2$. But x is in the pre-orbit of $2/3$, so $1/2$ would have to be as well. This isn't true, so $a_M(x)$ and hence the limit is non-zero.

3.4 Transients

For each initial point k, there is a finite sequence of values contained in the orbit before it reaches a periodic orbit. This is the transient of the orbit. Figure 10 plots the maximum transient over all initial points versus N and the average transient. The maximum transient is the top-most plot. The following figure, Figure 11 plots the natural log of the maximum and average transients versus the log of N. The linearity of the curves in this figure show that the curves in the previous figure follow a power law relation.

Figure 10: Log Average Transient vs. Log N

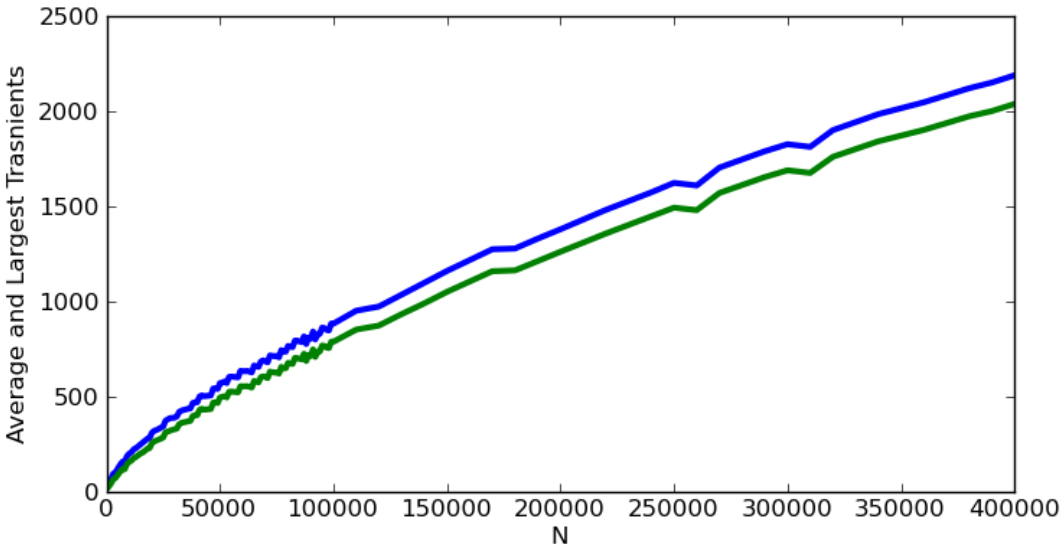

Figure 11: Log of Maximum and Average Transients vs. N

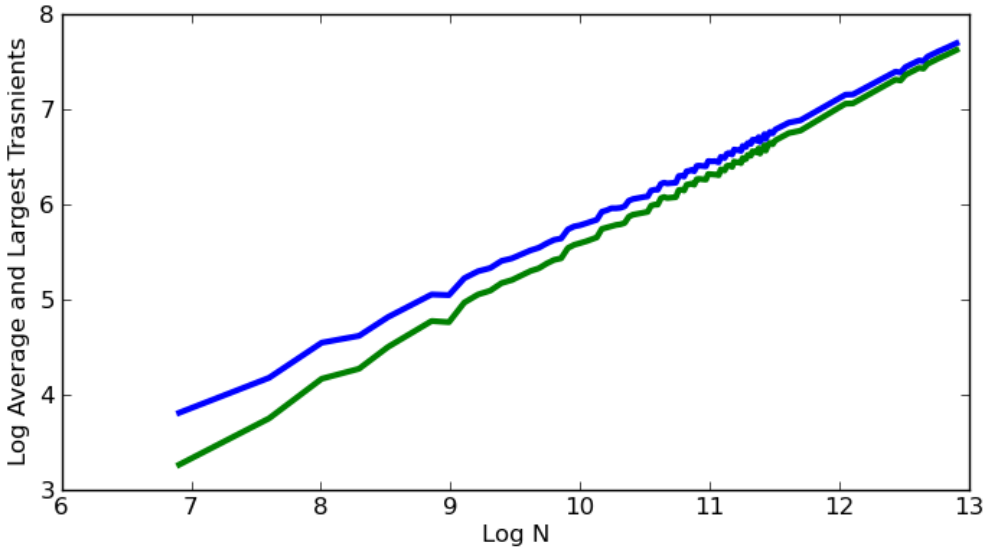

A linear fit for the maximum transient log-log graph gives

$$\log T_M(N) = 0.6577 \log N - 0.7984$$

with an r^2 value of 0.9992. The linear fit for the average is

$$\log T_A(N) = 0.6850 \log N - 1.2154$$

with an r^2 value of 0.9969. It appears that the average transient approaches the maximum transient as N gets large. Since the largest transient most likely resides in the largest basin, and the relative size of the largest basin appears to approach 1, this isn't too surprising. The author has no suggestions why the transients obey a roughly two-thirds power law.

3.5 Period doubling beyond $a = 3$.

The number of basins versus N was computed at three period doubling points after $a = 3$. Figure 12 plots the log (base 10) of the number of basins at the bifurcation points $a = 3$, $a = 3.449489743$, $a = 3.544090$, and $a = 3.564407$ versus the log (base 10) of N. The top-most plot corresponds to the first bifurcation, the one below to the second, and so on.

Figure 12: Number of basins of first four bifurcation points versus N

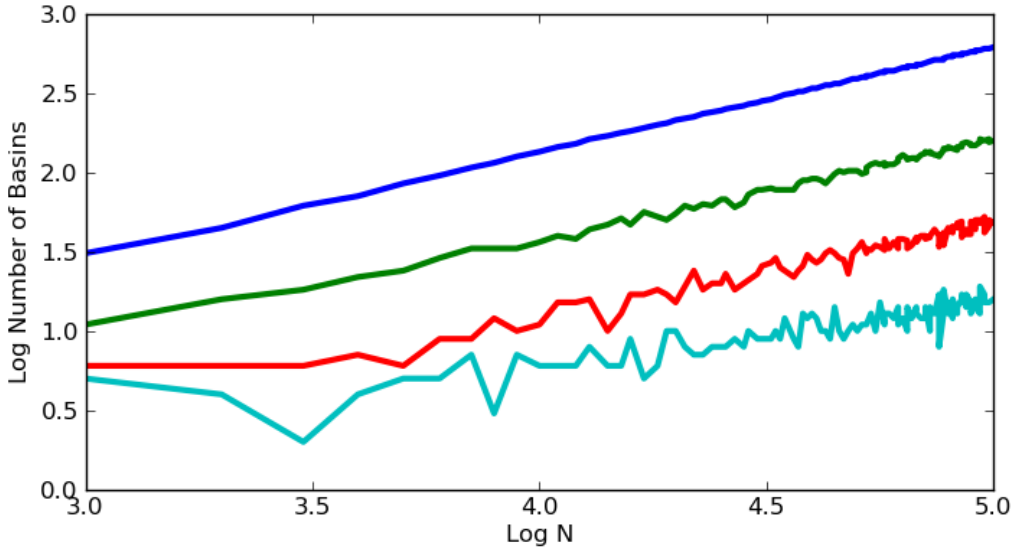

As seen, the number of basins roughly follow a two-thirds power law relation, except that later bifucation points have a smaller scaling coefficient. Additionally, the trend is noisier for later bifurcation points. The apparent two-thirds relation suggests that the 2^nth iterates are cubic near the periodic points. The noisiness is perhaps due to the increased sensitivity to the parameter a and the greater complexity of the map coming from the introduction of larger periodic orbits.

4 Floating Point Calculations at $a = 3$

It is of interest to compare the numerical nuances of floating point numbers with fixed point numbers. With floating point numbers, the spacing between adjacent numbers is not uniform. Rather, the closer to zero, the better the precision. Using single floating point precision, at the initial point $x_0 = 0.5$, the orbit under the logistic map at $a = 3$ heads into a numerically induced period two orbit of

$$x_0 = 0.668151 \quad \text{and} \quad x_1 = 0.665176.$$

If this is anything like the fixed point case, the initial point 0.5 should head to the largest period two orbit. This difference between the points in the periodic orbit is approximated by $2/\sqrt[3]{36N}$, according to (4). Near $x = 2/3$ with single precision, the spacing of points is uniform. Since the mantissa is $2^{23} \approx 840,000$, take that to be N. Thus, we have

$$x_1 - x_0 \approx 2/\sqrt[3]{36 \cdot 2^{23}} = 0.002981.$$

For floating point calculations, the difference between the two points is 0.002975. This is in good agreement with the prediction of 0.002981, differing only by $0.000006 = 6 \cdot 10^{-6}$.

Using a spacing of 10^{-4}, the following orbit limit diagram in Figure 13, similar to Figure 6, was generated with single precision.

Figure 13: Orbit Limits for Single Floating Point Precision

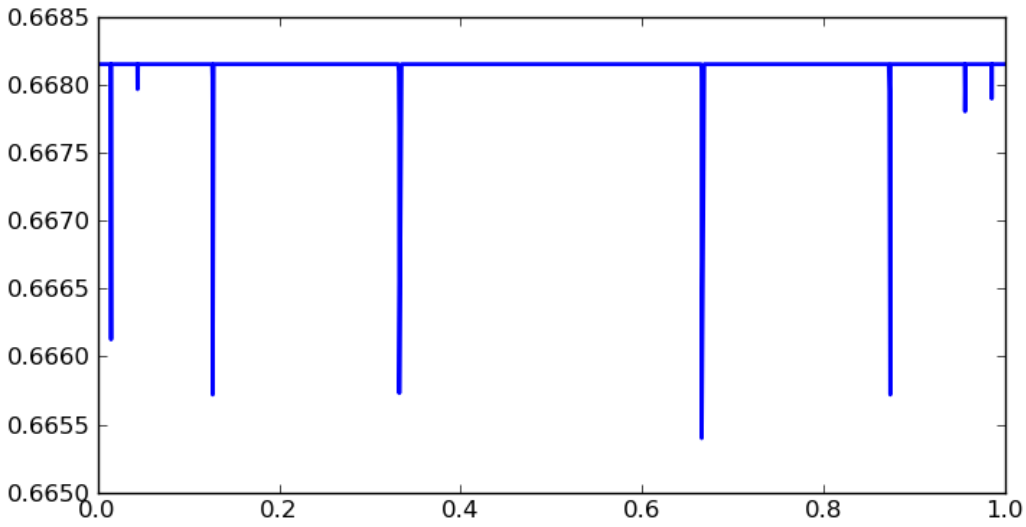

The figure suggests the number and location of induced period two orbits with the use of single precision floating point computations is similar to fixed point precision computations. This is because the spiked regions appear at similar locations. However, the length of the spikes do not have the same pattern as in Figure 6. They are also not symmetric about 1/2. This is not surprising, since the arrangement of points is not uniform. It would be interesting to investigate in detail how and why this differs with fixed point precision. For double precision, computations turn out to be lengthy and no graphs were obtained.

5 Results at $a = 4$ Chaos of the Logistic Map

The investigations in this section are rather introductory and exploratory–little analysis has been done.

5.1 Basins

The number of basins at $a = 4$ does not grow in the same way as it does at $a = 3$. It is more difficult to compute the number of basins for large N because the basins do not have an easily predicted orbit. Figure 14 plots the number of basins versus N. As seen, the plot is relatively constant, though rather jagged. Computations for N were stepped by 1,000, so the true graph would display an even greater fine structure. The author has no suggestions why this behavior is observed.

Figure 14: Number of Basins Versus N

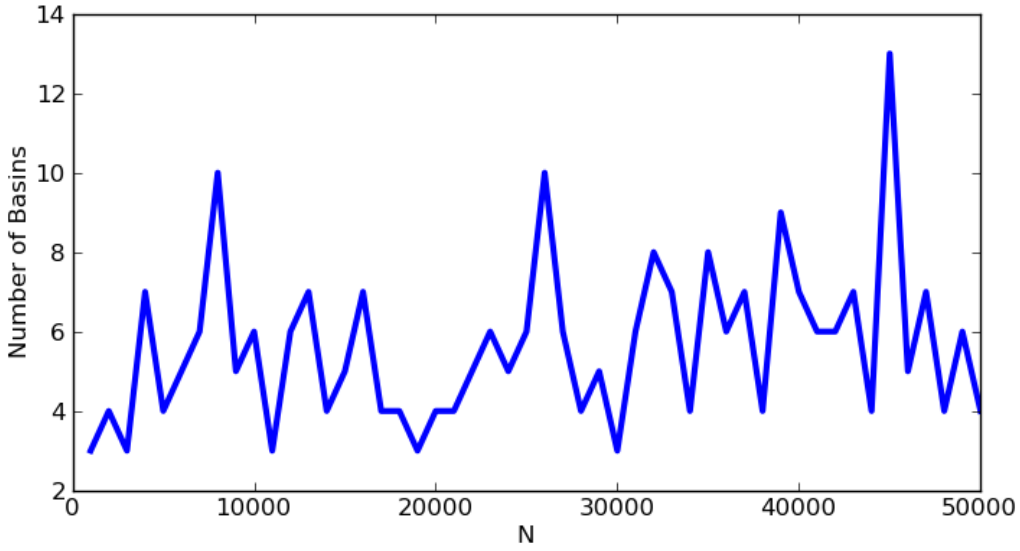

5.2 Transient and Period Length

Wang et al. produced graphs plotting the average period length found in the directed graph of the logistic map at $a = 4$ versus the number of approximating points using a similar model as (1) [4] (see also work done by [3]). They found that the average period versus $N = 10^h$ obeyed the power law

$$\bar{p} = 10^{-0.40} \cdot (10^h)^{0.47}. \tag{6}$$

Additionally, the found that the average transient length followed a near identical power law.

For small values of N, the numerically induced periodic orbits appeared to align with unstable periodic orbits. It is suspected that large numerically induced periodic orbits also correspond to unstable orbits, but this remains to be investigated carefully. It is possible that the application of the finite model is similar to measuring the fractal dimension of the set $\{x \in [0,1] \Big| f_4^{(n)}(x) = x \text{ for some } n\}$. The number of boxes used to cover the fractal, which is comparable to N, varies as a power law just as the period size varies as a power law. It is desirable to find explanations for these empirically observed powers laws, both with the period length and the transient length.

5.3 Overall Distribution of Periods

For a given N, there are often multiple periodic orbits in the directed graph. For instance, at $N = 156$, there exist five basins with period lengths of 1, 1, 2, 9, and 10. Sweeping over many values of N, period two orbits are a lot more common than period three orbits. Collecting all periodic orbits that arise in the graphs for some range of values of N, we can display the following distribution in Figure 15. For a given period length, it graphs the number of times a periodic orbit of that length occurs in range of directed graphs from $N = 10$ to $N = 1000$.

Figure 15: Histogram of Periods Occurring in Range of Graphs from $N = 10$ to $N = 1000$.

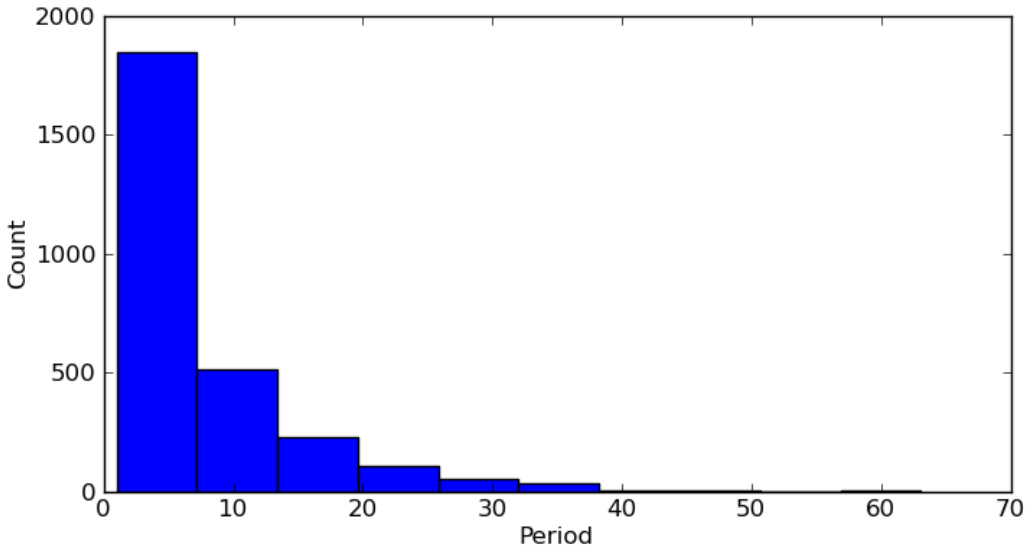

It is speculated that this distribution follows a power law. For instance, $p(k) = g(N)/k^{\alpha}$ for $k \in \mathbf{N}$. The normalizing factor is not simply N because the total number of periods is always greater than N. Instead, it is some function $g(N)$. Solving $p(k) = g(N)/k^{\alpha} = 1$, which implies $k = g(N)^{1/\alpha}$ suggests that near this value of N a periodic orbit of length k will be observed. If $g(N)$ obeys a power law, then this would line up with Wang et al's computations. Thus, it would be interesting to come up with an explanatory model of this observed distribution of periods.

5.4 Misiurewicz Conjecture

Misiurewicz conjectured that under the fixed point model of (1) with rounding to the nearest integer, there are an infinite number of values of N such that for the logistic map at $a = 4$ all orbits end up at zero [2]. In other words, the directed graph consists of only one basin.

Numbers starting from 10 below 100 where this occur are:

10, 13, 15, 19, 23, 25, 26, 27, 30, 37, 49, 50, 51, 57, 61, 70, 71, 74, 77, 79, 82, 85, 86, 87, 94, 98, ...

This conjecture could be proved if there is some method where given an N that has this property, an $N' > N$ can be produced that also has this property. A causal glance at the values of N where this occurs suggests a new N' roughly double a N might always exists. Also when investigating this conjecture, computing values of N where this property is satisfied gets difficult. Instead of starting at each initial point and calculating its orbit to see if it hits zero, perhaps calculating successive preimages

of 0 would result in a more efficient test of the conjecture. Finding an efficient algorithm for exploring this conjecture would be important.

It would be interesting to investigate this conjecture for other iterated maps. Work has been done on other maps investigating collapsing effects [1]. For instance, computations suggests that for the tent map the directed graph collapses for all N. This is probably easy to show analytically for $N = 2^h$, and it may be slightly harder to show it for all other values.

6 Error statistics

Consider the logistic map $f(x) = ax(1-x)$ and define

$$\delta_n = \frac{F^{(n)}(k)}{N} - f^{(n)}\left(\frac{k}{N}\right) \tag{7}$$

and ϵ_n as the most recent round-off error incurred when computing $F^{(n)}(k)$. First, note that it can be shown that

$$f(x+\delta) = f(x) + a\delta(1-2x-\delta). \tag{8}$$

Second, recall that

$$F(k) = Nf(k/N) + \epsilon \tag{9}$$

with the round-off error depending on k and N and satisfying $|\epsilon| < 1/2$. For convenience, let $x = k/N$. It follows that

$$\delta_{n+1} = \frac{F^{(n+1)}(k)}{N} - f^{(n+1)}(x) = \frac{1}{N}F\left[F^{(n)}(k)\right] - f^{(n+1)}(x) \tag{10}$$

By (7), we have

$$F^{(n)}(k) = N\left[f^{(n)}(x) + \delta_n\right] \tag{11}$$

Substituting this into (10), it turns out that

$$\begin{aligned}
\delta_{n+1} &= \frac{1}{N}F\left[N(f^{(n)}(x)+\delta_n)\right] - f^{(n+1)}(x) \\
&= \frac{1}{N}R\left[Nf(f^{(n)}(x)+\delta_n)\right] - f^{(n+1)}(x) \\
&= \frac{1}{N}\left[Nf^{(n+1)}(x) + a\delta_n N(1-2f^{(n)}(x)-\delta_n) + \epsilon_{n+1}\right] - f^{(n+1)}(x)
\end{aligned}$$

In conclusion, we obtain the recurrence relation

$$\delta_{n+1} = a\delta_n\left[1-2f^{(n)}(x)-\delta_n\right] + \epsilon_{n+1}/N. \tag{12}$$

This relation may be useful in analyzing the statistics of the errors computed. For instance, we can consider the maximum possible error under the "round to nearest integer" map as follows. Define

$$\Delta_n = \max|\delta_n| \text{ over } (\epsilon_1, \epsilon_2, \ldots, \epsilon_n) \in [-1/2, 1/2]^n. \tag{13}$$

What is

$$\Delta_1, \Delta_2, \Delta_3, \ldots$$

and $\lim_{n\to\infty}\Delta_n$? We know that both the computational orbit and the true orbit are contained in the unit interval, so practically, the sequence is bounded by 1. Analytically, is this the case? If not, can useful information, perhaps about the transients, be obtained? Future study would include trying to answer these questions.

6.1 Distribution Plots

The following figure (Figure 16) displays distributions, for different parameter values of the logistic map, of δ_1, δ_2, δ_3 as k is varied. A value of $N = 100,000$ was used. Interestingly, typical of all N and a, the distribution of δ_1 appears to be uniform. The distributions of δ_2 and δ_3 are more complicated. It is possible the recurrence relation (12) would be useful in deriving a probability distribution function for each of them based on the assumption that the round-off error is a uniform random variable.

Figure 16: Distribution plots of error statistics, $N = 100,000$

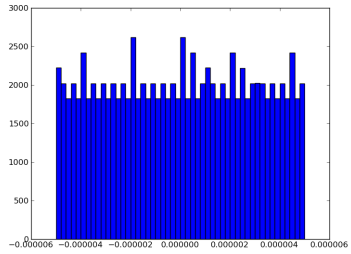

$a = 2,\ n = 1$

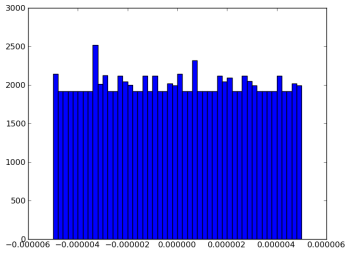

$a = 3,\ n = 1$

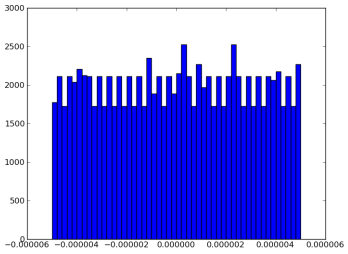

$a = 4,\ n = 1$

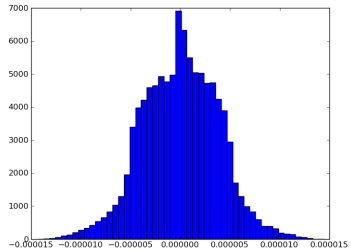

$a = 2,\ n = 2$

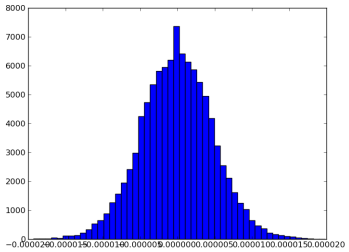

$a = 3,\ n = 2$

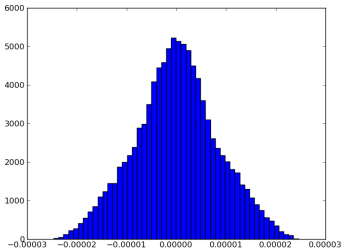

$a = 4,\ n = 2$

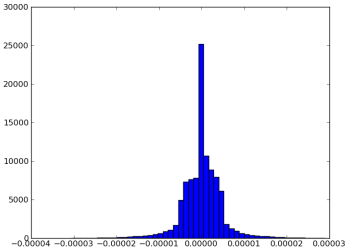

$a = 2,\ n = 3$

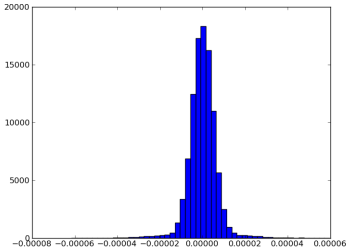

$a = 3,\ n = 3$

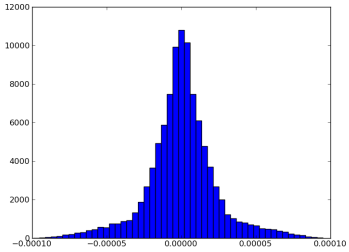

$a = 4,\ n = 3$

7 Conclusion

The rich dynamical behavior of iterated maps is just as rich, if not more, when analyzing them under finite computational models. While it may not be strictly true, chaotic maps tend to become less chaotic under a finite model, since all orbits are eventually periodic, while stable maps like the logistic map at $a = 3$ exhibit more complicated behavior under the model.

Future work would include more careful analysis of the $a = 3$ and $a = 4$ logistic maps, among analysis of other bifurcation points and chaotic points. Attempts to prove the Misiurewicz Conjecture would be interesting. The error statistics could be more thoroughly studied along with other rounding schemes. Additionally, other iterated maps, including higher dimensional maps, could be analyzed.

8 Acknowledgments

Thank you to my advisor Jim Swift, the Research Experience for Undergraduates (REU) coordinator John Neuberger, the Northern Arizona University (NAU) Math Department, and the National Science Foundation (NSF) for funding the REU program.

Additionally, the open sources tools C++, python, the python image library, the matplotlib python library, and graphviz proved reliable and useful.

References

[1] P. Diamond, M. Suzuki, P. Kloeden, and P. Pokrovskii. Statistical properties of discretizations of a class of chaotic dynamical systems. *Computers and Mathematics with Applications*, 31(11):83 – 95, 1996.

[2] Michal Misiurewicz. Discrete logistic map. `www.math.iupui.edu/~mmisiure/open/mm.pdf`, August 2010.

[3] T. Miyazaki, S. Araki, and S. Uehara. Period and link length of logistic map over integers. In *Information Theory and Its Applications, 2008. ISITA 2008. International Symposium on*, pages 1 –5, 7-10 2008.

[4] S. Wang, W. Liu, H. Lu, J. Kuang, and G. Hu. Periodicity of Chaotic Trajectories in Realizations of Finite Computer Precisions and its Implication in Chaos Communications. *International Journal of Modern Physics B*, 18:2617–2622, 2004.